Journal of Hazardous Materials 186 (2011) 1335–1342

Contents lists available at ScienceDirect

Journal of Hazardous Materials

journal homepage: www.elsevier.com/locate/jhazmat

Novel zwitterionic inorganic–organic hybrids: Synthesis of hybrid adsorbents and their applications for Cu^{2+} removal

Qiang Dong, Junsheng Liu*, Long Song, Guoquan Shao*

Key Laboratory of Membrane Materials & Processes, Department of Chemical and Materials Engineering, Hefei University, 373 Huangshan Road, Hefei, 230022, China

ARTICLE INFO

Article history:
Received 5 October 2010
Received in revised form 3 December 2010
Accepted 3 December 2010
Available online 10 December 2010

Keywords:
Zwitterionic hybrids
Cu^{2+} removal
Kinetics
Zwitterionic process
Adsorption

ABSTRACT

A series of zwitterionic hybrid adsorbents were prepared via the ring-opening polymerization of pyromellitic acid dianhydride (PMDA) and N-[3-(trimethoxysilyl)propyl] ethylene diamine (TMSPEDA), and a subsequent zwitterionic process as well as sol–gel reaction. Their applications for Cu^{2+} removal by adsorption were performed. FTIR spectra confirmed the step products. TGA revealed that the initial decomposition temperature (IDT) of these zwitterionic hybrid adsorbents could arrive at near 150 °C. DSC showed that T_g values decreased with an increase in PMDA content in the hybrid matrix. Ion-change capacity (IEC) revealed that the cation-exchange capacities (CIECs) and anion-exchange capacities (AIECs) of these hybrid adsorbents were within the range of 9.13–11.49 and 4.97–6.28 mmol g^{-1}, respectively. Meanwhile, the CIECs and AIECs exhibit an opposite change trend as PMDA content increases. Adsorption experiment indicated that their adsorptions for Cu^{2+} ions followed Lagergren second-order kinetic model, surface adsorption and intraparticle diffusion mechanisms might be the major process. These findings demonstrated that they are promising absorbents for the separation and recovery of Cu^{2+} ions from contaminated water.

1. Introduction

Inorganic–organic hybrid polymeric materials or membranes containing functionalized ionic groups have become more and more attractive because of their structural flexibility, mechanical stability, functional group performances and potential applications in some harsh environments, such as high temperature and strongly oxidizing atmosphere [1–3]. For preparing these hybrid polymers, silane-coupling agent (or alkoxyorganosilane) is usually directly used as hybrid precursor for sol–gel process to obtain the inorganic moiety in the hybrid matrix [4]. However, these silicones can also be incorporated into the hybrid matrix via the polymerization of alkoxysilane with reactive organic monomer [5,6].

Presently, various innovative approaches are designed to synthesize the functionalized hybrid polymeric materials or membranes. Among these, zwitterionic hybrid polymer or material has been deserved increasing attention [7,8]. This is because such type of hybrid polymer has an advantage over the pure organic or inorganic materials not only in molecular structure, but also in performance characteristics. Especially, its unique pendant-side structure of opposite ionic groups arranged on the molecular chains will permit its application in the removal of heavy metal ions from water via electrostatic effect, indicating promising application prospects in wastewater treatment and heavy metal recovery [9,10].

Recently, an effort was made to prepare and characterize zwitterionic hybrid polymer and membranes, several novel routes to these zwitterionic hybrids were proposed in our laboratory [10–12]. One route was initiated via sol–gel process of hybrid precursor [10], in which the ionic groups (–COOH) were created by the ring-opening of 1,4-butyrolactone. Another route based on the effect of steric hindrance of phenyl groups and sol–gel process was designed and developed [11], in which the silicone was incorporated into the hybrid matrix via the ring-opening polymerization of pyromellitic acid dianhydride (PMDA) and phenylaminomethyl trimethoxysilane (PAMTMS); and the –COOH groups were fabricated through preventing the cyclodehydration of –N– and –COOH groups in the adjacent polymer chains. Meanwhile, the adsorption and desorption behaviors of these zwitterionic hybrid polymers for Cu^{2+} and Pb^{2+} were evaluated for the recovery of heavy metal ions from aqueous solution [12], confirming their promising applications in the removal and recovery of heavy metal ions from wastewater. Our continuing interest in such zwitterionic hybrids stimulates us to make further effort.

To develop new approach to zwitterionic hybrid polymer used as an adsorbent and investigate its application for the removal of heavy metal ions, herein, a novel route to synthesize zwitterionic hybrid adsorbents was designed. Compared with the previous

* Corresponding authors. Tel.: +86 551 2158439; fax: +86 551 2158437.
E-mail addresses: jsliu@hfuu.edu.cn (J. Liu), sgq@hfuu.edu.cn (G. Shao).

0304-3894/$ – see front matter © 2010 Elsevier B.V. All rights reserved.
doi:10.1016/j.jhazmat.2010.12.012

Table 1
Composition of the prepared zwitterionic hybrid adsorbents.

Sample	PMDA (mol)	TMSPEDA (mol)	BL (mol)
A	0.1	0.1	0.01
B	0.2	0.1	0.01
C	0.3	0.1	0.01
D	0.4	0.1	0.01

articles [10,11], the particularity of this new route is that: (1) the silicone was incorporated into the hybrid matrix via ring-opening polymerization of PMDA and N-[3-(trimethoxysilyl)propyl] ethylene diamine (TMSPEDA), (2) the ion pairs (i.e. anion- and cation-exchange groups) produced by the ring-opening of 1,4-butyrolactone with secondary amine groups were arrayed on both sides of the polymer chains, establishing a pendant-side structure. Moreover, their adsorptions for Cu^{2+} ions will be evaluated as a model for the separation and recovery of heavy metal ions from contaminated water.

2. Experimental

2.1. Materials

N-[3-(trimethoxysilyl)propyl] ethylene diamine (TMSPEDA, purity: ≥95.0%) was purchased from Silicone New Material Co. Ltd. of Wuhan University (Wuhan, China) and used without further purification. Pyromellitic acid dianhydride (PMDA, purity: ≥99.5%) and 1,4-butyrolactone (BL, purity: ≥97.0%) were purchased from National Pharmaceutical Group Corp. of China (Shanghai, China) and used as received. Other reagents were of analytical grade.

2.2. Synthesis of zwitterionic hybrid adsorbents

The zwitterionic hybrid adsorbents were synthesized by reacting proper PMDA with TMSPEDA at room temperature in DMF solution (the composition of zwitterionic hybrid adsorbents was listed in Table 1). The procedure can be briefly described as follows.

Firstly, stipulated PMDA was dissolved in proper DMF solution and stirred vigorously for 1 h at room temperature; and then stoichiometric TMSPEDA solution was added dropwise into the above-prepared DMF mixed solution within 1 h. Subsequently, the DMF mixed solution was stirred vigorously for additional 30 min to conduct ring-opening polymerization of PMDA and TMSPEDA. After that, a homogeneous sol, i.e. hybrid precursor, could be obtained. Thirdly, the zwitterionic process of ring-opening of a lactone reagent with the secondary amine groups situated on the polymer chains was carried out by adding stipulated amount of 1,4-butyrolactone (BL) to the above-prepared hybrid precursor for 24 h to create ion pairs (i.e. anion- and cation-exchange groups). During this process, sol–gel reaction occurs between Si and O to produce the Si–O–Si bonds in the hybrid precursor. Finally, the obtained product was washed and dried at 70 °C for 12 h to obtain the final zwitterionic hybrid adsorbent.

2.3. Sample characterizations

FTIR spectra of products were obtained using a Shimadzu FTIR-8400S Fourier transform infrared spectrometer in the region of 4000–400 cm^{-1} at a resolution of 0.85 cm^{-1}.

TGA and DSC thermal degradation process of the prepared samples was investigated using a Netzsch STA 409 PC/PG thermogravimetry analyzer, under nitrogen flow using a heating rate of 20 K/min from 10 to 400 °C.

Ion-exchange capacity (IEC) of the above-prepared zwitterionic hybrid adsorbents was determined using a Shenghan CIC-200 ion chromatography (Qingdao, China) operated at a flow-rate of 0.3 mL/min for anions, equipped with a self-regenerating anion micromembrane suppressor; and 0.7 mL/min for cations. The procedure is as follows: 1.0 g powder sample was immersed in a large amount of deionized water for 24 h and washed several times to remove the impurity. Subsequently, the polymer was converted to Cl^- and Na^+ ionic form by immersing it in an aqueous NaCl solution (20 mL, 0.1 mol dm^{-3}) for 24 h. Both anion-exchange capacities (AIECs) and cation-exchange capacities (CIECs) values could thus be calculated from the difference of ionic concentration before and after ion substitute. To reduce the experimental errors, the experiment was carried out in triplicate and the mean values of thrice testing from these independent experiments were selected as the final results. The measuring error is estimated to be within 5%.

2.4. Adsorption experiment

The adsorption experiment of zwitterionic hybrid adsorbents for Cu^{2+} ions was conducted in similar way as described in the previous articles [11,12]. The procedure can be described briefly as follows: about 1.0 g of particle sample was immersed in 0.01 mol dm^{-3} $Cu(NO_3)_2$ for 24 h at pH 4, and then taken out and washed by deionized water. In the remaining solution, 10% KI solution was added; subsequently, an aqueous $Na_2S_2O_3$ solution (0.05 mol dm^{-3}) was used to titrate iodine so that the residual Cu^{2+} ions can be measured.

The adsorption capacity ($q_{Cu^{2+}}$) of Cu^{2+} ions is calculated as follows:

$$q_{Cu^{2+}} = \frac{(C_0 - C_R)V}{W} \quad (1)$$

where V is the volume of aqueous $Cu(NO_3)_2$ solution (mL), C_0 and C_R are the concentrations of initial and remaining $Cu(NO_3)_2$, respectively (mol dm^{-3}), W is the weight of hybrid adsorbent (g).

The effect of solution temperature on the adsorption of Cu^{2+} ions was performed to determine optimal temperature condition. For adsorption kinetic studies, the prepared sample was immersed in 0.01 mol dm^{-3} aqueous $Cu(NO_3)_2$ solution for different adsorption times at 45 °C and pH 4. The adsorption data were analyzed using Lagergren first-order, Lagergren second-order kinetic and intraparticle diffusion models. Meanwhile, error analysis was conducted and the standard deviation is indicated in the parameter calculation.

3. Results and discussion

3.1. Synthesis of zwitterionic hybrid adsorbents

As mentioned in the experimental section, the zwitterionic hybrid adsorbents were synthesized via the ring-opening polymerization of PMDA and TMSPEDA to incorporate inorganic Si into the hybrid matrix. Subsequently, ion pairs located on the polymer chains were produced by the ring-opening of BL with secondary amine groups in the hybrid precursor. Since PMDA is an acid anhydride and TMSPEDA is a primary amine, ring-opening polymerization between them is easily conducted. Scheme 1 presents the reaction steps.

As shown in Scheme 1, three reaction steps were involved: step 1 was the ring-opening polymerization of PMDA and TMSPEDA, and the step product was the hybrid precursor. The main product of this step was determined by the molar ratio of PMDA and TMSPEDA. Step 2 was the zwitterionic process of ring-opening of BL with the secondary amine groups in the hybrid precursor to produce the ion pairs. Step 3 was the hydrolysis and condensation of alkoxysilane to create the hybrid network. In this step, the alkoxysilane hydrolyzed and condensed, and produced the Si–O–Si bonds through sol–gel

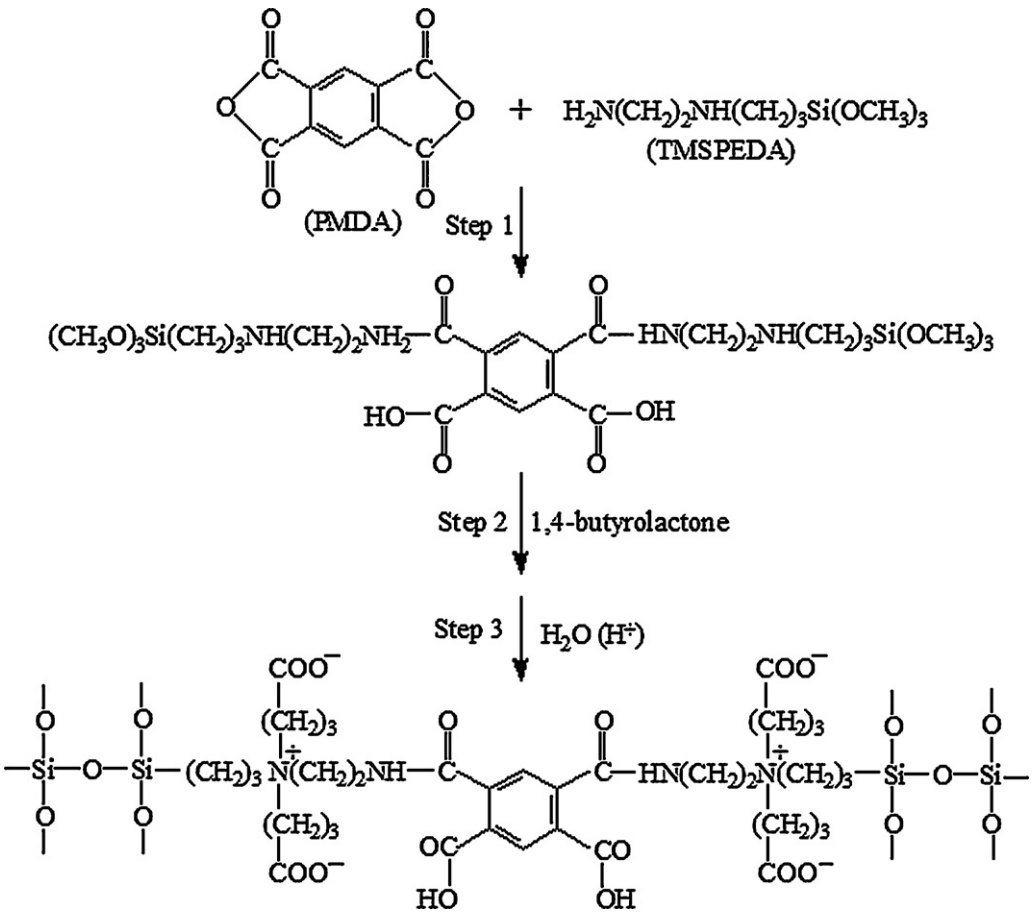

Scheme 1. The preparing route of zwitterionic hybrid adsorbents, step 1 is the ring-opening polymerization of PMDA and TMSPEDA to produce the hybrid precursor, step 2 is the zwitterionic process of 1,4-butyrolactone with amine groups to create ion pairs in the polymer chains, step 3 is the hydrolysis and condensation of alkoxysilane by sol–gel reaction.

reaction. In addition, taking the structure of ionic groups into account, it can be seen that the above-prepared hybrid adsorbents contains both anion- and cation-exchange groups, while these ionic groups are arranged on the pendant-side chains; consequently, it is a zwitterionic one.

Note that, the hydrolysis and condensation of alkoxysilane in Step 3 possibly occurred ahead of Step 2 or both steps might occur simultaneously during the synthesis of hybrid adsorbents. However, it is less important in this case because such behavior does not affect any of the final product and its property. In the synthesis of zwitterionic hybrid adsorbents, our major concern is the creation of Si–O–Si and Si–O–C bonds in the hybrid matrix via hydrolysis and condensation of alkoxysilane rather than the formation sequence of step products.

3.2. FTIR spectra and the confirmation of step products

To confirm the step reactions described in Scheme 1, FTIR spectroscopy of samples A–D was performed and presented in Fig. 1.

As shown in Fig. 1, it can be noted that curves (a)–(d) have similar change trends except the intensity of peaks. The strong absorption peak at near 1720 cm^{-1} was the stretching vibration of C=O in –COOH groups. The band at 3400 cm^{-1} was the stretching vibration of –OH groups. The absorption peaks at 2950 cm^{-1} could be ascribed to the C–H stretching of CH_3 and CH_2 groups. The peak around 1100 cm^{-1} was the overlapping of asymmetric stretching vibration of Si–O–Si, Si–O–C and C–O–C bonds from alkoxysilane [4,13]. The band near 1260 cm^{-1} was the stretching vibration of C–N in the samples. Meanwhile, the peaks at 1400 and 1608 cm^{-1} were, respectively, in the range of 1300–1430 cm^{-1} and 1550–1610 cm^{-1}, which should be ascribed to the stretching vibration of COO^- groups [14].

Comparing the curves (a)–(d) in Fig. 1, it can be found that the intensity of the band at 1100 cm^{-1} for the C–O–C stretching vibration increases a little as the PMDA content in the investigated samples increases, revealing an increasing content of organic ingredient. Moreover, it can also be found that the band at 1860 and 1774 cm^{-1}, which should be ascribed to the stretching vibration of C=O in acid anhydride [15], appeared in curves (c) and (d),

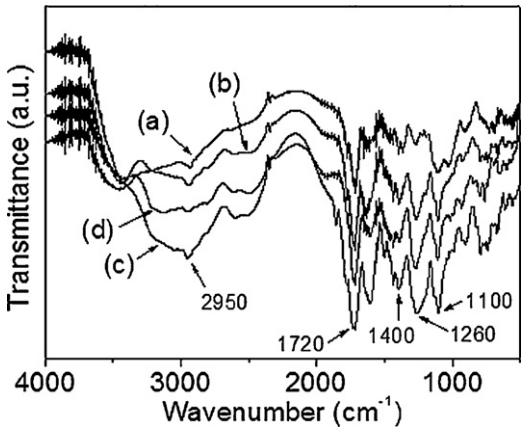

Fig. 1. FTIR spectra of (a–d) denoted the samples A–D, respectively.

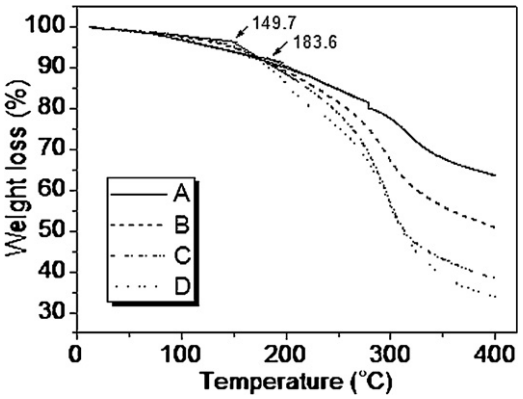

Fig. 2. TGA curves of samples A–D.

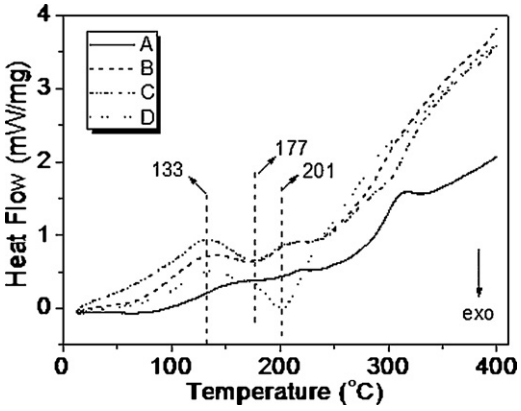

Fig. 3. DSC curves of samples A–D.

suggesting that there exists excess amount of PMDA in the prepared samples and the ring-opening polymerization of PMDA and TMSPEDA was unfulfilled. Based on these findings, it can be concluded that the ring-opening polymerization had occurred during the synthesis of hybrid adsorbents, further corroborating the reactions illustrated in Scheme 1.

3.3. TGA analysis

Thermal stability is a major concern for hybrid polymeric materials. To have an insight into the thermal degradation behaviors of the prepared zwitterionic hybrid adsorbents, TGA thermal analysis was carried out and shown in Fig. 2. Meanwhile, the thermal analysis data in TGA curves are listed in Table 2.

As shown in Fig. 2, for samples A–D, their change trends in weight loss are similar and three degradation steps can be clearly found. However, the initial decomposition temperature (IDT) [16] (i.e. tangent rule, only two IDT points were labeled in TGA curves because of the overlapping and crossing of tangential lines) and thermal degradation temperature at 5 and 10% weight loss (T_5 and T_{10}) indicated different change trends. For example, for individual sample, T_5 and T_{10} improved with an increase in the weight loss. Whereas, for different samples, the IDT value decreases from samples A to C and then increases for sample D, which is clearly opposite the change trend in T_5. In contrast, T_{10} exhibits a downward trend, (i.e. it decreases from 198.4, 192.6, 189.3 to 183.6 °C for samples A–D, respectively), demonstrating that the thermal stability of these samples decreases with an increase in the incorporation of organic PMDA into the hybrid matrix (Table 2). In addition, it can be seen that the weight loss of these samples increases rapidly when the degradation temperature exceeds T_{10}, suggesting that the decomposition has been accelerated. Moreover, it can be observed that the residual SiO_2 weight at 400 °C (R_{400}) are 63.5, 50.8, 38.3 and 33.9% for samples A–D, respectively (cf. Table 2), implying a decrease of inorganic ingredients in these samples. This finding is agreement with the theoretical expectation (i.e. the residual weight decreases with an increase in the organic ingredient of a polymer).

Table 2
Thermal analysis data of samples obtained from TGA curves.

Sample	IDT (°C)[a]	T_5 (°C)[b]	T_{10} (°C)[b]	R_{400} (wt%)[c]
A	183.6	129.8	198.4	63.5
B	157.1	147.8	192.6	50.8
C	149.7	151.4	189.3	38.3
D	172.3	134.4	183.6	33.9

[a] Initial decomposition temperature.
[b] Thermal degradation temperature of 5 and 10% weight loss in TGA curves, respectively.
[c] Residual weight at 400 °C in TGA curves.

The weight loss below T_{10} was the removal of bonded water and solvent in the samples. Whereas the sharp weight loss beyond T_{10} can be assigned to the decomposition of organic ingredients and the production of silica, which is consistent with the result reported in an article [17], in which it is stated that when a polymer contains a pendant active methoxysilane group, the methoxy groups are eliminated to form crosslinked Si–O–Si bonds in the early stages of heating, resulting in the creation of silica.

To explain the above phenomena, special attention will be paid to the following dominating factors. One can be ascribed to the increases in both the amount of organic ingredient and the flexibility of these samples. As shown in Table 2, the residual weight of SiO_2 in the samples decreases from samples A to D as PMDA content increases; consequently, the R_{400} values indicate a downward trend. Another might be attributed to the hydrophilicity of carboxylic groups. From samples A to D, the amount of ion pairs grafted on the polymer chains increases. Especially, more amount of carboxylic groups grafted on the polymer chains is produced, thus the hydrophilicity of the zwitterionic hybrid adsorbents will accordingly be elevated. As a result, the decomposition of functionalized ionic groups becomes easy and the thermal degradation temperature decreases accordingly.

Note that, for sample D, the change trend in TDI and T_5 is inconsistent with those of samples A–C. The reason can be ascribed to the impact of crosslinking between the organic and inorganic moieties, and the formation of silica hybrid network as extra amount of ion pairs are introduced into the polymer chains, which will lead to the formation of intimate molecular structure and the elevation of thermal degradation temperature [17]. In addition, the electrostatic attraction between the ion pairs will also be responsible for the improved thermal stability of sample D, blocking its further thermal decomposition.

3.4. DSC study

Glass transition temperature (T_g) is usually related to the structural properties of a polymer. Understanding T_g will favor the recognition of the crystallization transformation of a polymer from a rigid material to a flexible one. To investigate the crystallization transformation of the prepared zwitterionic hybrid adsorbents, DSC study was carried out and the related curves are presented in Fig. 3.

As shown in Fig. 3, it can be observed that there exist only one endothermic and one exothermic peak for respective DSC curve. As reported [18], in DSC curves, the single or multiple endothermic peaks are the crystal melting; whereas the exothermic peak can be considered as the crystallization. Consequently, the T_g value for samples A–D is at near 318.7, 135.0, 133.0 and 131.6 °C, respectively, which indicates a downward trend as the PMDA con-

Table 3
Ion-exchange capacities (IECs) of the prepared zwitterionic hybrid adsorbents.

	Sample			
	A	B	C	D
CIECs (mmol g^{-1})	9.55	9.13	9.83	11.49
AIECs (mmol g^{-1})	6.28	5.92	4.97	5.82
Ratio of CIEC/AIEC	1.52	1.54	1.97	1.97
Net charge (mmol g^{-1})[a]	3.27	3.21	4.86	5.67

[a] Net charge = CIEC − AIEC.

tent increases, suggesting the transformation of crystalline form. Meanwhile, the melting point temperature (T_m) for samples A–D centered at 328.7, 175.3, 177.1 and 201.4 °C, respectively, which was elevated as PMDA content increases except that of sample A. The upward trend in T_m can be ascribed to an increase in the pendant-side chain and the further formation of hybrid network because extra amount of PMDA is incorporated into the zwitterionic hybrid adsorbents. Furthermore, the electrostatic attraction between the ion pairs will also be responsible for the elevated T_m.

Clearly, these findings demonstrate the influence of PMDA content and the amount of ion pairs on the thermal behaviors of zwitterionic hybrid adsorbents.

3.5. Ion-exchange capacity (IEC)

Ion-exchange capacity (IEC) is a helpful tool to recognize the ion-exchange ability of hybrid polymers containing functionalized ionic groups. To determine the charge amount of anion- and cation-exchange groups in the above-prepared zwitterionic hybrid adsorbents, IEC values were measured and shown in Table 3.

As shown in Table 3, it can be seen that the cation-exchange capacities (CIECs) and anion-exchange capacities (AIECs) of these hybrid adsorbents were within the range of 9.13–11.49, 4.97–6.28 mmol g^{-1}, respectively, demonstrating that these hybrid adsorbents contain both cation- and anion-exchange groups. Moreover, it can also be seen that the CIEC values increase with the increasing content of PMDA in the hybrid adsorbents except that of sample B, suggesting that the incorporation of PMDA into the polymer matrix can increase their ion-exchange abilities. In contrast, the AIEC values decreases with an increasing content of PMDA except that of sample C, revealing an opposite trend with CIECs.

Several factors might be responsible the above-mentioned change trend. One is related to the content of –COOH in the polymer chains. As presented in Table 1, from samples A to D, more amount of –COOH groups are grafted on the polymer chains when the ring-opening reaction of epoxide occurred with the elevating content of PMDA; resulting in an increase in CIEC values. Another can be ascribed to the existence of epoxy groups in the PMDA moiety, which are easily converted to –COOH in the presence of water because of its acid anhydride property [18]; thus it will increase the amount of –COOH in the polymer chains, resulting in an increase in CIECs. In addition, the ring-opening of BL will also make some contributions to the increasing CIECs.

As for the downward trend in AIECs, it is reasonable if the following dominating factors are considered. One factor might be related to the electrostatic attraction between the $–COO^-$ and $–N^+–$ groups because of its pendant-side structure, leading to a decrease in the amount of exchangeable $–N^+–$ groups as stated in an article [11]. Another can be attributed to the embedment position of $–N^+–$ groups in the polymer chains, and the larger difference of net charge of anionic and cationic groups. As shown in Scheme 1, the $–N^+–$ groups were surrounded by $–COO^-$ groups, thus the accessibility of anionic ions to the positive charge sites will be blocked and decreased. As a result, the exchangeable amount of count-ion to the $–N^+–$ groups is relatively lower, resulting in lower AIECs from samples A to D.

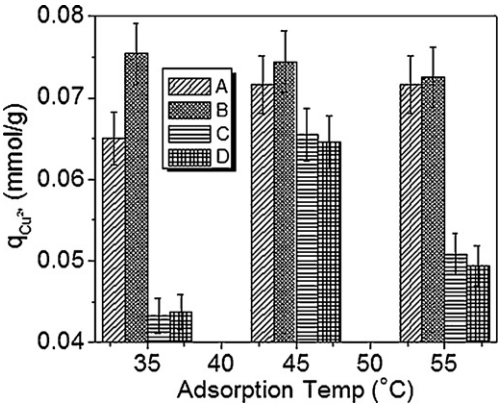

Fig. 4. Adsorption capacity of Cu^{2+} ions *vs.* solution temperature, the concentration of aqueous $Cu(NO_3)_2$ solution was 0.01 mol dm^{-3} for 24 h.

Moreover, taking the difference of net charge into account, it can be noted that they demonstrate the same upward trend as that of CIEC: increase from samples A to D and sample B has the lowest one (cf. Table 3). However, if the ratio of CIEC and AIEC is considered, they reveal two relatively fixed values, i.e. 1.52, 1.54, 1.97 and 1.97 from samples A to D, respectively. This finding suggests that the quantities of anionic and cationic groups in the polymer chains are produced in pairs, corroborating the reaction described in Scheme 1.

It should be emphasized that the larger difference of net charge, which mainly reveals the cation-exchange property, will benefit their applications in the removal of heavy metal ions, such as Cu^{2+} and Pb^{2+} ions, from wastewater via counter-ion adsorption and ion-exchange because of the effect of electrostatic attraction between the ionic groups (cf. Table 4, hereinafter). Consequently, these zwitterionic hybrid adsorbents expect to be potentially applied to absorb or separate heavy metal ions from contaminated water. To confirm such consideration, adsorption experiment for Cu^{2+} ions was carried out and discussed later.

3.6. Adsorption study

To have an insight into the adsorption properties of the above-prepared zwitterionic hybrid adsorbents, adsorption experiment was conducted using Cu^{2+} as a model of heavy metal ions. The dominating factors examined include adsorption temperature and adsorption time. The adsorption data were analyzed using Lagergren first-order, Lagergren second-order kinetic and intraparticle diffusion models to study the adsorption kinetic properties of Cu^{2+} ions on these zwitterionic hybrid adsorbents.

3.6.1. Effect of solution temperature

It is well known that solution temperature is an important factor affecting the adsorption behavior of heavy metal ions in aqueous solution. To select optimal temperature for Cu^{2+} adsorption, the effect of solution temperature on the adsorption capacity of Cu^{2+} ions was investigated and presented in Fig. 4.

Clearly, solution temperature at 45 °C is more suitable for Cu^{2+} adsorption. Consequently, 45 °C was chosen as the adsorption temperature of aqueous solution to study the adsorption behaviors of Cu^{2+} ions on the above-prepared zwitterionic hybrid adsorbents, hereafter.

3.6.2. Adsorption kinetics

Fig. 5 presents the adsorption kinetic curves of Cu^{2+} ions, i.e. the relationship between adsorption capacity and adsorption time.

Table 4
Lagergren second-order kinetic model parameters for Cu^{2+} adsorption.

Sample	k_2 (h g mmol^{-1})	h[a] (h g mmol^{-1}	q_{exp} (mmol g^{-1})	q_{cal} (mmol g^{-1})	R^2	SSE
A	13.195	6.968×10^{-2}	6.925×10^{-2}	7.267×10^{-2}	0.992	3.42×10^{-3}
B	40.215	2.299×10^{-1}	7.492×10^{-2}	7.561×10^{-2}	0.999	6.90×10^{-4}
C	18.560	7.888×10^{-2}	6.548×10^{-2}	6.519×10^{-2}	0.994	2.90×10^{-4}
D	19.513	8.067×10^{-2}	6.454×10^{-2}	6.430×10^{-2}	0.994	2.40×10^{-4}

[a] Initial adsorption rate (h) = $k_2 q_e^2$.

It is interesting to find that the adsorption capacity of Cu^{2+} ions on samples A–D decreases with an increase in CIEC values, suggesting that Cu^{2+} adsorption on these samples is related to the content of ionic groups and lower CIECs may be more conduce to the adsorption of Cu^{2+} ions on these zwitterionic hybrid adsorbents. The reason possibly is ascribed to the pendant-side structure of carboxylic groups on the polymer chains and the larger difference of net charge, resulting in lower electrostatic attraction between the metal ions and ionic groups.

It is well accepted that Lagergren adsorption kinetic model is a helpful tool to describe the adsorption property of a species [19]. Its first-order and second-order kinetic equation can be linearly expressed as Eqs. (2b) and (3b), respectively.

$$q_t = q_e(1 - e^{-k_1 t}) \tag{2a}$$

or

$$\log(q_e - q_t) = \log q_e - \frac{k_1}{2.303} t \tag{2b}$$

$$q_t = \frac{q_e^2 k_2 t}{(1 + q_e k_2 t)} \tag{3a}$$

or

$$\frac{t}{q_t} = \frac{1}{k_2 q_e^2} + \frac{t}{q_e} \tag{3b}$$

where k_1 and k_2 are the first-order and second-order rate constant, respectively (h g mmol^{-1}); q_t and q_e are the adsorption capacity of Cu^{2+} ions at time t and at equilibrium state, respectively (mmol g^{-1}).

Moreover, error analysis was used to determine the most suitable kinetic model. The sum of error squared (SSE) between the predicted values and the experimental data can be calculated by the following equation [20]:

$$\mathrm{SSE} = \frac{\sqrt{\sum_{i=1}^{N} (q_{exp} - q_{cal})^2}}{N} \tag{4}$$

where q_{exp} and q_{cal} are the experimental and calculated adsorption capacity of metals, respectively (mmol g^{-1}). N is the number of measurements.

The Lagergren adsorption kinetic model for Cu^{2+} adsorption was calculated and presented in Fig. 6. It is interesting to find that the Lagergren first-order model for Cu^{2+} adsorption on samples A–D exhibited poor regression coefficient (R^2) (the data were not presented in the text); suggesting that Cu^{2+} adsorption on these samples cannot be described by Lagergren first-order kinetic equation. However, it can be noted that the linear regression coefficient (R^2) of Lagergren second-order model fitted well for Cu^{2+} adsorption (cf. Table 4). Based on these data, it can be concluded that Cu^{2+} adsorption on these zwitterionic hybrid adsorbents followed Lagergren second-order kinetic model.

Furthermore, by comparison the Lagergren second-order kinetic model parameters for Cu^{2+} adsorption in Table 4, it can be found that the second-order rate constant (k_2) and initial adsorption rate (h) of Cu^{2+} ions increase from samples A to D, which reveals the same upward trend as these of CIEC and net charge except those of sample B (cf. Table 3, hereinbefore). This outcome demonstrates that IECs of zwitterionic hybrid adsorbents really have an effect on Cu^{2+} adsorption.

3.6.3. Effect of intraparticle diffusion

The effect of intraparticle diffusion on adsorption rate can be calculated based on the relation of adsorption capacity and time, which usually is expressed as Eq. (5) [21]:

$$q_t = x_i + k_p t^{0.5} \tag{5}$$

where q_t is the adsorbed amount (mmol g^{-1}) at time t, k_p is the intraparticle diffusion rate constant (mmol g^{-1} h$^{-0.5}$) and x_i is the intercept of straight line, which is related to the boundary layer thickness. When metal ions are adsorbed by an adsorbent, the metal ions transport from the solution through the interface between the solution and the adsorbent into the pores of the particles. It is now well accepted that if the plot of q_t *vs.* $t^{0.5}$ gives a straight line, the adsorption process is solely controlled by intraparticle diffusion. If the data exhibit multi-linear plots, however, two or more steps will influence the adsorption process [21,22].

Fig. 7 illustrated the intraparticle diffusion curves for Cu^{2+} adsorption in this case. As shown in Fig. 7, it can be found that the adsorption of Cu^{2+} ions on samples A–D is non-linear over the range of adsorption time and three steps are involved: the rapid

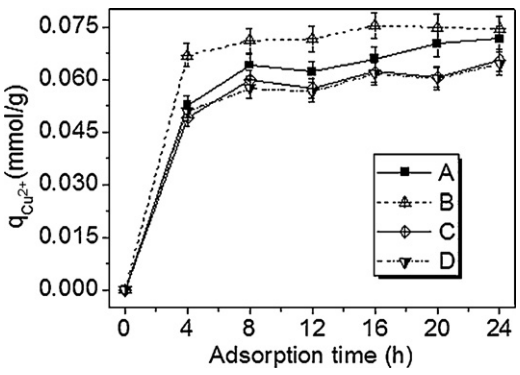

Fig. 5. Adsorption capacity of Cu^{2+} ions *vs.* adsorption time, the concentration of aqueous $Cu(NO_3)_2$ solution was 0.01 mol dm^{-3} at 45 °C and pH 4.

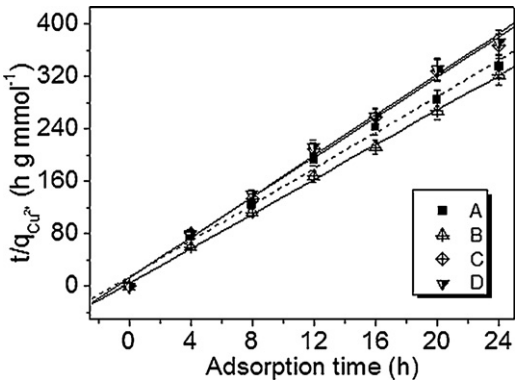

Fig. 6. Lagergren second-order kinetic model for Cu^{2+} adsorption on samples A-D.

Table 5
Diffusion rate constants for Cu^{2+} adsorption.

Sample	Interface diffusion		Intraparticle diffusion	
	K_{id} (mmol g^{-1} $h^{-0.5}$)	K_p (mmol g^{-1} $h^{-0.5}$)	K_{p1} (mmol g^{-1} $h^{-0.5}$)	K_{p2} (mmol g^{-1} $h^{-0.5}$)
A	2.637×10^{-2}	5.93×10^{-3}	5.92×10^{-3}	6.35×10^{-3}
B	3.345×10^{-2}	2.76×10^{-3}	3.90×10^{-3}	1.05×10^{-3}
C	2.448×10^{-2}	4.65×10^{-3}	5.81×10^{-3}	3.56×10^{-3}
D	2.542×10^{-2}	4.15×10^{-3}	4.79×10^{-3}	3.04×10^{-3}

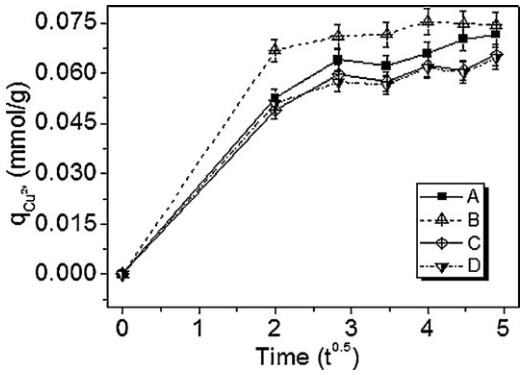

Fig. 7. Intraparticle diffusion curves for Cu^{2+} adsorption on samples A–D.

interface diffusion from 0 to 4 h; subsequently the intraparticle diffusion (increased slowly and approached equilibrium) [20,23]. This finding suggests that Cu^{2+} adsorption on these samples is not solely governed by intraparticle diffusion [in the case of linear fitting, they exhibited poor regression coefficient (R^2), i.e. R^2 is 0.850, 0.748, 0.823 and 0.814 for samples A–D, respectively]; diffusion-controlled adsorption mechanisms might be the major process as reported in articles [21,22].

To further explore the adsorption mechanism, diffusion rate constants for Cu^{2+} adsorption are calculated and listed in Table 5. It can be noted that interface diffusion rate (slope K_{id}, which was calculated in the time range of 0–4 h) is much higher than intraparticle diffusion rate (slope $K_{p,}$ which was calculated in the time range of 4–24 h), implying that intraparticle diffusion is the major rate-limiting step because it is the slow step in adsorption process. Meanwhile, the intraparticle diffusion rate of second step (slope K_{p2}, which was calculated in the time range of 16–24 h), in which the intraparticle diffusion comes to slow down and reaches to the final equilibrium, is lower than the intraparticle diffusion rate of first one (slope K_{p1}, which was calculated in the time range of 4–16 h), in which the intraparticle diffusion is established and accelerated. These results indicate that the adsorption process is controlled by surface adsorption and intraparticle diffusion.

Furthermore, by comparison the data of K_{id} with those of AIECs, it can be found that they reveal the same change trend except that of sample B, further demonstrating the influence of ionic groups on the behaviors of Cu^{2+} adsorption.

The theoretical explanation to this phenomenon can be ascribed to the pendant-side structure and different amounts of ionic groups existed in the polymer backbone, leading to the change of adsorption mechanism.

4. Conclusions

A new route to synthesize zwitterionic hybrid adsorbents was proposed. These zwitterionic hybrid adsorbents were prepared via the ring-opening polymerization of PMDA and TMSPEDA; subsequently, a ring-opening of BL and sol–gel reaction. TGA analysis displayed that the thermal degradation temperature decreased as the PMDA content increases. IEC measurements revealed that the CIECs and AIECs of these hybrid adsorbents were within the range of 9.13–11.49, 4.97–6.28 mmol g^{-1}, respectively. Meanwhile, the ratio of CIEC and AIEC centered on fixed values, which can be ascribed to the existence of ion pairs in PMDA moiety. Adsorption experiment revealed that Cu^{2+} adsorption on these zwitterionic hybrid adsorbents followed the Lagergren second-order kinetic model. Meanwhile, the effect of intraparticle diffusion reveals that Cu^{2+} adsorption on these samples is not solely governed by intraparticle diffusion. It is indicated that surface adsorption and intraparticle diffusion is the major process. These findings are very meaningful in the separation and recovery of heavy metal ions from wastewater.

Acknowledgements

This project was financially supported by the Natural Science Foundation of China (No. 21076055), Significant Foundation of Educational Committee of Anhui Province (No. ZD2008002-1), Anhui Provincial Natural Science Foundation (No. 090415211) and the Opening Project of Key Laboratory of Solid Waste Treatment and Resource Recycle (SWUST), Ministry of Education (No. 09zxgk03). Special thanks will be given to the two anonymous reviewers for their insightful comments and suggestions.

References

[1] T.W. Xu, Ion exchange membranes: state of their development and perspective, J. Membr. Sci. 263 (2005) 1–29.
[2] J.Y. Luo, C.M. Wu, Y.H. Wu, T.W. Xu, Diffusion dialysis of hydrochloride acid at different temperatures using PPO-SiO_2 hybrid anion exchange membranes, J. Membr. Sci. 347 (2010) 240–249.
[3] Y. Tao, L. Ye, J. Pan, Y. Wang, B. Tang, Removal of Pb(II) from aqueous solution on chitosan/TiO_2 hybrid film, J. Hazard. Mater. 161 (2009) 718–722.
[4] H. Ramadan, A. Ghanem, H. El-Rassy, Mercury removal from aqueous solutions using silica, polyacrylamide and hybrid silica–polyacrylamide aerogels, Chem. Eng. J. 159 (2010) 107–115.
[5] Y.H. Wu, C.M. Wu, T.W. Xu, Y.X. Fu, Novel anion-exchange organic–inorganic hybrid membranes prepared through sol–gel reaction of multi-alkoxy precursors, J. Membr. Sci. 329 (2009) 236–245.
[6] C.-S. Chang, H.-S. Ni, S.-Y. Suen, W.-C. Tseng, H.-C. Chiu, C.P. Chou, Preparation of inorganic–organic anion-exchange membranes and their application in plasmid DNA and RNA separation, J. Membr. Sci. 311 (2008) 336–348.
[7] P. Innocenzi, E. Miorin, G. Brusatin, A. Abbotto, L. Beverina, G.A. Pagani, M. Casalboni, F. Sarcinelli, R. Pizzoferrato, Incorporation of zwitterionic push–pull chromophores into hybrid organic–inorganic matrixes, Chem. Mater. 14 (2002) 3758–3766.
[8] W.J. Liang, C.P. Wu, C.Y. Hsu, P.L. Kuo, Synthesis, characterization, and proton-conducting properties of organic–inorganic hybrid membranes based on polysiloxane zwitterionomer, J. Polym. Sci., Part A: Polym. Chem. 44 (2006) 3444–3453.
[9] J.S. Liu, Y. Ma, Y.P. Zhang, G.Q. Shao, Novel negatively charged hybrids. 3. Removal of Pb^{2+} from aqueous solution using zwitterionic hybrid polymers as adsorbent, J. Hazard. Mater. 173 (2010) 438–444.
[10] J.S. Liu, T.W. Xu, Y.X. Fu, Fundamental studies of novel inorganic–organic charged zwitterionic hybrids. 2. Preparation and characterizations of hybrid charged zwitterionic membranes, J. Membr. Sci. 252 (2005) 165–173.
[11] J.S. Liu, Y. Ma, T.W. Xu, G.Q. Shao, Preparation of zwitterionic hybrid polymer and its application for the removal of heavy metal ions from water, J. Hazard. Mater. 178 (2010) 1021–1029.
[12] J.S. Liu, X.H. Wang, T.W. Xu, G.Q. Shao, Novel negatively charged hybrids. 1. Copolymers: preparation and adsorption properties, Sep. Purif. Technol. 66 (2009) 135–142.
[13] C.M. Wu, T.W. Xu, M. Gong, W.H. Yang, Synthesis and characterizations of new negatively charged organic–inorganic hybrid materials. Part II. Membrane preparation and characterizations, J. Membr. Sci. 247 (2004) 111–118.

[14] M.J. Ayora-Cañada, B. Lendl, Study of acid–base titration of succinic and malic acid in aqueous solution by two-dimensional FTIR correlation spectroscopy, Vib. Spectrosc. 24 (2000) 297–306.
[15] S.M. Wu, T. Hayakawa, R. Kikuchi, S.J. Grunzinger, M. Kakimoto, Synthesis and characterization of semiaromatic polyimides containing POSS in main chain derived from double-decker-shaped silsesquioxane, Macromolecules 40 (2007) 5698–5705.
[16] S.V. Kumar, S. Prasannakumar, B.S. Sherigara, B.S.R. Reddy, T.M. Aminabhavi, *N*-vinylpyrrolidone and 4-vinyl benzylchloride copolymers: synthesis, characterization and reactivity ratios, J. Macromol. Sci. Part A: Pure Appl. Chem. 45 (2008) 821–827.
[17] S.-S. Hou, P.-L. Kuo, Function and performance of silicone copolymers. 3. Synthesis and properties of a novel siliconized acrylic monomer containing three reactive sites, Macromol. Chem. Phys. 200 (1999) 2501–2507.
[18] J.-H. Chang, D.-K. Park, K.J. Ihn, Polyimide nanocomposite with a hexadecylamine clay: synthesis and characterization, J. Appl. Polym. Sci. 84 (2002) 2294–2301.
[19] G.P. Kumar, P.A. Kumar, S. Chakraborty, M. Ray, Uptake and desorption of copper ion using functionalized polymer coated silica gel in aqueous environment, Sep. Purif. Technol. 57 (2007) 47–56.
[20] Y. Hao, M. Chen, Z. Hu, Effective removal of Cu (II) ions from aqueous solution by amino-functionalized magnetic nanoparticles, J. Hazard. Mater. 184 (2010) 392–399.
[21] A.A. Atia, A.M. Donia, A.M. Yousif, Removal of some hazardous heavy metals from aqueous solution using magnetic chelating resin with iminodiacetate functionality, Sep. Purif. Technol. 61 (2008) 348–357.
[22] L. Zhao, H. Mitomo, Adsorption of heavy metal ions from aqueous solution onto chitosan entrapped CM-cellulose hydrogels synthesized by irradiation, J. Appl. Polym. Sci. 110 (2008) 1388–1395.
[23] S. Goswami, U.C. Ghosh, Studies on adsorption behaviour of Cr(VI) onto synthetic hydrous stannic oxide, Water SA 31 (2005) 597–602.